Dalton Transactions

Accepted Manuscript

This article can be cited before page numbers have been issued, to do this please use: M. Koepf, J. J. Bergkamp, A. Teillout, M. J. Llansola Portoles, G. Kodis, A. L. Moore, D. Gust and T. A. Moore, *Dalton Trans.*, 2017, DOI: 10.1039/C6DT04647A.

This is an Accepted Manuscript, which has been through the Royal Society of Chemistry peer review process and has been accepted for publication.

Accepted Manuscripts are published online shortly after acceptance, before technical editing, formatting and proof reading. Using this free service, authors can make their results available to the community, in citable form, before we publish the edited article. We will replace this Accepted Manuscript with the edited and formatted Advance Article as soon as it is available.

You can find more information about Accepted Manuscripts in the author guidelines.

Please note that technical editing may introduce minor changes to the text and/or graphics, which may alter content. The journal's standard Terms & Conditions and the ethical guidelines, outlined in our author and reviewer resource centre, still apply. In no event shall the Royal Society of Chemistry be held responsible for any errors or omissions in this Accepted Manuscript or any consequences arising from the use of any information it contains.

ROYAL SOCIETY OF CHEMISTRY

rsc.li/dalton

View Article Online
DOI: 10.1039/C6DT04647A

Journal Name

ARTICLE

Design of porphyrin-based ligands for the assembly of [*d*-block metal:calcium] bimetallic centers

Received 00th January 20xx,
Accepted 00th January 20xx

DOI: 10.1039/x0xx00000x

www.rsc.org/

Matthieu Koepf,[a]† Jesse J. Bergkamp,[a]‡ Anne-Lucie Teillout,[a]• Manuel J. Llansola-Portoles,[a]± Gerdenis Kodis,[a] Ana L. Moore,[a]* Devens Gust,[a]* and Thomas A. Moore[a]*

The association of different metals in stable, well-defined molecular assemblies remains a great challenge of supramolecular chemistry. In such constructs, the emergence of synergism, or cooperative effects between the different metal centers is particularly intriguing. These effects can lead to uncommon reactivity or remarkable physico-chemical properties that are not otherwise achieveable. For example, the association of alkaline or alkaline-earth cations and transition metals is pivotal for the activity of several biomolecules and human-made catalysts that carry out fundamental redox transformations (water oxidation, nitrogen reduction, water-gas shift reaction, etc.). In many cases the precise nature of the interactions between the alkaline-earth cations and the redox-active transition metals remains elusive due to the difficulty of building stable molecular heterometallic assemblies that associate transition metals and alkaline or alkaline-earth cations in a controlled way. In this work we present the rational design of porphyrin-based ligands possessing a second binding site for alkaline-earth cations above the porphyrin macrocycle primary complexation site. We demonstrate that by using a combination of crown ether and carboxylic acid substituents suitably positioned on the periphery of the porphyrin, bitopic ligands can be obtained. The binding of calcium, a typical alkaline-earth cation, by the newly prepared ligands has been studied in detail and we show that a moderately large binding constant can be achieved in protic media using ligands that possess some degree of structural flexibility. The formation of Zn-Ca assemblies discussed in this work is viewed as a stepping stone towards the assembly of well defined molecular transition metal-alkaline earth bimetallic centers using a versatile organic scaffold.

Introduction

Synthetic ligands designed to assemble hetero-metallic complexes are key to various fields of research, including molecular recognition, molecular devices, and catalysis.[1, 2] In the latter case, the association of different metals within a well-defined organic framework can lead to the appearance of cooperative behavior, or synergism, between the metallic centers, sometimes giving rise to unique reactivity patterns and unprecedented catalytic activities.[3-10]

One important aspect of hetero-metallic synergism, observed in both natural and synthetic systems, is the modulation of transition-metal based redox processes induced by redox-inactive alkaline or alkaline-earth cations.[11-49] In nature, the oxygen evolving complex (OEC) found in Photosystem II of photosynthetic organisms offers a remarkable example of such synergism; the association of a calcium ion with four redox-active manganese centers is critical for the enzyme's activity for water-oxidation.[17, 19, 31, 41, 50-53]

In the area of synthetic chemistry, some notable examples of such synergism have been described as well. Since 1910, iron doped with potassium has been known as a superior catalyst for the Haber-Bosch process, providing higher selectivity and activity than pure iron in the reduction of molecular nitrogen to ammonia.[11] Following this early example, the alteration of the performance of heterogeneous catalysts upon doping with alkaline or alkaline-earth cations has been explored for platinum-catalyzed water-gas shift reactions,[20, 23] manganese-catalyzed water oxidation,[22, 32, 34, 54] and other major industrially relevant processes.[12, 13, 18]

The study of synergistic effects between transition-metal molecular complexes and alkaline, alkaline-earth, or other redox-inactive cations in homogeneous conditions has

[a] *School of Molecular Sciences, Arizona State University, Tempe, AZ 85287, USA.*
† Current address: Laboratoire de Chimie et Biologie des Métaux, CEA–CNRS–UGA UMR 5249, 17 rue des Martyrs, Bât. K', 38054 Grenoble Cedex 9, France
‡ Current address: Department of Chemistry, California State University, 9001 Stockdale Highway, Bakersfield, CA, 93311, USA.
• Current address: Laboratoire de Chimie Physique d'Orsay, Université Paris-Sud Bât. 349 - Campus d'Orsay, 15, avenue Jean Perrin, 91405 Orsay Cedex, France.
± Current address: Institute for Integrative Biology of the Cell (I2BC), CEA, CNRS, Université Paris-Sud, Université Paris-Saclay, F-91198, Gif-sur-Yvette cedex, France.
Electronic Supplementary Information (ESI) available: [detailed synthetic procedure and characterization of the ligands, additional ^{1}H NMR information, details of the fluorescence anisotropy measurements, and UV vis titrations]. See DOI: 10.1039/x0xx00000x

View Article Online
DOI: 10.1039/C6DT04647A

attracted attention as well. Early studies highlighted the effects of magnesium salts on the product distribution and kinetics of iron-porphyrin mediated electro-catalytic carbon dioxide reduction[14] as well as the enhancement of the oxygen transfer rate between chemically generated tetraamido manganese-oxo complexes and unsaturated substrates in the presence of alkali and alkaline-earth cations.[15] Following these examples, systematic studies were undertaken to investigate the control of the rates and stoichiometry of electron transfer between organic or organometallic substrates and iron-, manganese- and cobalt-oxo and peroxo complexes by the addition of scandium, calcium and other redox-inactive cations.[21, 26, 28, 30, 42, 44, 45, 55] In the case of catalytically active iron and manganese complexes, the alteration of the high-valent metal-oxo derivatives' properties by the addition of redox inactive cations was found to greatly affect the mechanisms of oxidative C-H bond cleavage, sulfoxidation, and epoxidation reactions of benchmark substrates.[33, 35, 36, 42, 43, 46, 56] Following these lines, the influence of calcium, barium, and strontium cations on the kinetics of direct oxygen activation by various iron(II), and manganese(II) complexes was investigated as well.[29, 38, 45, 57] Collectively, these examples highlight the potential of redox-inactive cations to control specific catalytic processes in homogeneous conditions. However, in these examples, the association of the different metals does not result from the specific coordination of the cations within a well-defined ligand scaffold. Thus, the resulting heterometallic assemblies are essentially transient species, and the control and fine-tuning of their reactivity remains challenging.

This limitation has recently been circumvented by the introduction of ingenious ligands and assembly procedures, developed mainly in the context of manganese chemistry. These procedures permitted the preparation of well-defined heterometallic $Mn_3O_4A_n$ clusters (with A = Na, Ca, Sr, Sc, Zn, Y, La, Ce, Nd, Eu, Gd, Tb, Dy, Yb, or Lu, and n = 1, 2).[25, 39, 40, 48, 58, 59] These constructs provided a direct way to probe the modulation of the redox properties of the manganese centers upon doping the clusters with redox-inactive cations.[25, 39, 40, 48] A linear correlation between the reduction potential of the clusters and the Lewis acidity of the redox-inactive cations was demonstrated.[25, 39, 40, 48] However such a simple correlation is not universal for assemblies of transition metals and redox-inactive cations within a well-defined scaffold.[60] In addition, the reactivity of calcium- and scandium-doped Mn_3O_4A clusters towards oxo transfer reactions on phosphines was tested as a first step towards the investigation of the catalytic activity of such species.[37]

Some of the aforementioned studies[25, 58, 59] attracted particular attention in the context of water oxidation, through introduction of classes of synthetic models precisely mimicking the core of the OEC.[61] Other than these remarkable examples, only a limited number of studies have reported the preparation of discrete alkaline-earth/manganese hetero-metallic assemblies,[27, 62-71] and like the examples discussed above, most of them rely on the incorporation of oxo-bridges within their structures. The labile nature of such assemblies in aqueous conditions when submitted to a redox cycle has been highlighted.[27] Lability is partly due to the use of manganese-oxo bridges as a major structural element of the heterometalic assemblies. The stability of such bridges is indeed closely related to the redox state of the manganese ions and the pH of the solution.[72] Thus the development of robust, well-defined hetero-metallic complexes that associate manganese (or other transition metals) and alkaline or alkaline-earth cations remains challenging in aqueous and more generally in protic media. The limited availability of appropriate ligand hampers the extensive investigation of alkaline-earth / transition metal synergism in catalytic processes.

In this manuscript, we present the design of novel organic scaffolds able to promote the association of first-row transition metals and alkali-earth metals within compact, well-defined structures in protic media. Moreover, in order to overcome some of the stability issues discussed previously, we have focused on the development of assemblies that do not feature structural metal-oxo bridges. The synthesis and characterization of various ligands will be presented as well as the results of ^{1}H-NMR spectroscopy, UV-*Vis* spectroscopy, and time resolved fluorescence anisotropy studies that investigate the metal binding properties of the ligands in solution. We will focus on the complexation of Zn^{2+} and Ca^{2+} as model transition-metal and alkaline-earth cations, respectively. Because these metal ions lack unpaired electrons, NMR spectroscopy can be used for characterization and binding studies.

Results and discussion

Design of porphyrin-based *N,O*-bitopic ligands

Porphyrins and related tetrapyrrolic macrocycles are known to strongly coordinate most of the transition-metals within an N_4-chelating motif.[73, 74] Stable manganese, iron, cobalt, and nickel porphyrins are commonly prepared and used as active catalysts for various reactions such as carbon dioxide reduction, oxygen reduction, water oxidation, and oxygen transfer reactions.[75-81] The *beta*- and *meso*-positions of

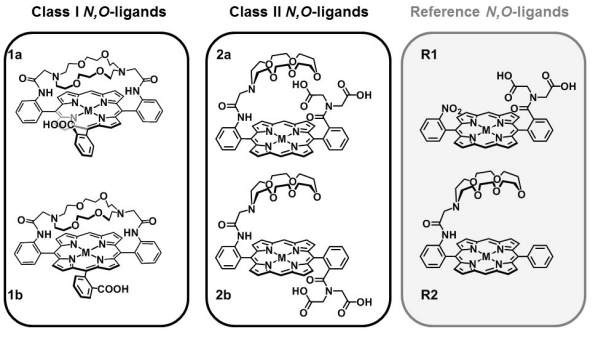

Figure 1: Bitopic *N,O*-ligands studied in this work. Class I ligands (M = H_2) are based on a strapped architecture imposing strong geometrical constraints on the oxygen-rich binding site. Class II ligands (M = Zn) offer a more flexible architecture for the oxygen-rich binding site. Reference ligands (M = Zn) feature the main binding elements of class-II ligands grafted onto the N_4-binding site in a non-interacting fashion.

View Article Online
DOI: 10.1039/C6DT04647A

the porphyrin macrocycle are readily available for synthetic modifications, making the latter a useful scaffold for building multi-topic ligands around a primary N_4-chelating motif. It is noteworthy that alkaline-earth metals do not form stable porphyrin complexes in protic media, with the exception of magnesium.[82] In fact, alkaline-earth cations, and particularly calcium, exhibit a strong preference for oxygen-rich ligands.[83-85] Therefore we investigated different strategies for building a second coordination site for alkaline-earth cations using oxygen donors positioned directly above the porphyrin macrocycle. Since crown ethers and carboxylic acid groups are among the most widely used ligands for the complexation of alkaline-earth metals in protic media,[85-89] we have investigated combinations of these binding motifs around the porphyrin scaffold in order to prepare ligands exhibiting two highly differentiated binding sites, *i.e.* bitopic *N,O*-ligands.

A variety of crown ether appended porphyrins have already been reported. Two main designs can be distinguished, wherein the crown ether moiety is: *i)* grafted on the periphery of the tetrapyrrolic macrocycle forming a simple dangling secondary binding site or, *ii)* anchored at two points on the porphyrin, forming a strap above the N_4 chelating site.[90] The functionalization of the porphyrin macrocycle with carboxylic acid groups has been reported as well,[81, 91-95] and was found to be a viable strategy for preparing heterobimetallic complexes.[96] To the best of our knowledge, only one type of carboxylate functionalized porphyrin has been tested for calcium binding and it led to the aggregation of the macrocycles in solution.[93] It is worth noting that the functionalization of a porphyrin with a crown ether bearing a hanging carboxylic acid group was described as well, without any indication of the ability of this specific ligand to form alkaline-earth (heterometallic) complexes.[97]

Inspired by these precedents, we defined two classes of ligands combining carboxylic acids and polyether functionalities distributed on the periphery of the porphyrin macrocycle as promising *N,O*-bitopic ligands (Figure 1). The architectures were designed to possess either a completely preorganized (rigid) or a rather flexible oxygen-rich binding site.

Class I ligands feature a fairly rigid (highly preorganized) structure in which the crown ether is covalently attached to the porphyrin macrocycle via two opposite *meso*-positions to form a strap above the tetrapyrrolic N_4-binding site (Figure 1). The introduction of a 2-carboxyphenyl substituent on a third *meso*-position of the porphyrin can lead to two thermally stable atropisomers (**1a** and **1b**) due to the high energy barrier for rotation about the bonds joining the *ortho*-substituted aryl rings to the porphyrin macrocycle. Compound **1a** is the primary target because for this atropisomer, the carboxylic acid is orientated towards the crown ether and is expected to favor the *endo* coordination of alkaline-earth cations within the cavity formed by the crown ether strap and the porphyrin.

Class II ligands were designed to offer a much more flexible (adaptable) oxygen-rich binding site. For this purpose, a crown ether and a dicarboxylic acid moiety were grafted on two opposite *meso*-positions of the porphyrin macrocycle. As in the case of the class I ligands two thermally stable atropisomers can be expected (**2a** and **2b**) depending on the relative orientation of the substituents with respect to the plane of the porphyrin. Compound **2a** is expected to allow the crown ether and the carboxylic acids to act in a cooperative way to coordinate alkaline-earth cations, and position them above the porphyrin plane.

Synthesis of the ligands

The synthetic route to class I ligands was derived from a strategy reported by Conte *et al.*,[98] and is discussed in the supporting information (*cf.* SI, section 1.2).

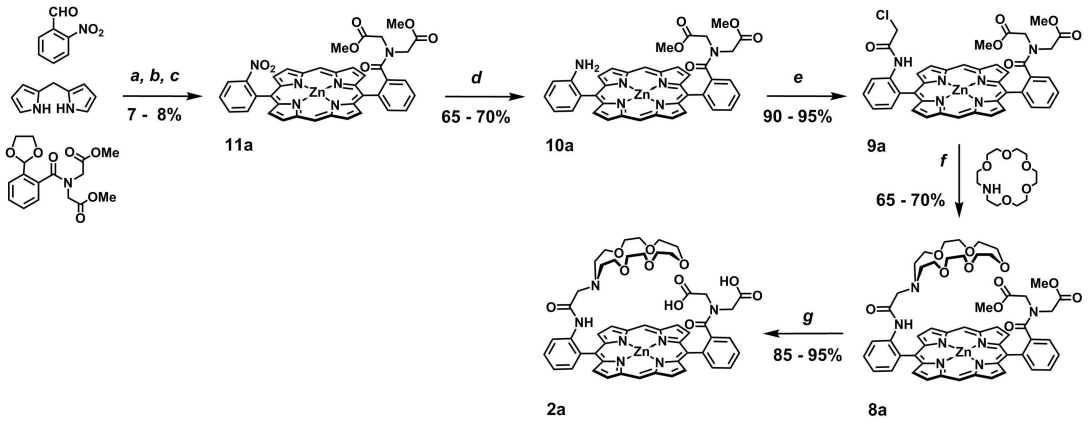

Scheme 1: Synthetic scheme for ligand **2a**. The same synthetic strategy was followed to prepare ligand **2b**, starting from the atropisomer **11b** (for which the nitro group and diester substituents are facing towards the two opposite sides of the porphyrin macrocycle). *a)* $BF_3.Et_2O$, CH_3Cl, Ar, RT; *b)* DDQ (dichloro-dicyano quinone), CH_2Cl_2 RT; *c)* $Zn(OAc)_2$, $CHCl_3$, MeOH, RT; *d*) Zn, AcOH (acetic acid), CH_2Cl_2, Ar, RT; *e)* $ClCH_2COCl$, K_2CO_3, CH_2Cl_2, Ar, O°C – RT; *f)* EtOH, Ar, 70°C; *g)* KOH, EtOH, H_2O, Ar, 50°C.

View Article Online
DOI: 10.1039/C6DT04647A

Class II ligands were obtained following the general synthetic strategy depicted in Scheme 1. The precursor porphyrin (**11**) was obtained as a mixture of two atropisomers from the statistical acid-catalyzed condensation of dipyrrylmethane with 2-nitrobenzaldeyhde and the acetal derivative of dimethyl 2,2'-(2-formylbenzamido)diacetate. Each atropisomer of the desired mixed-porphyrin, **11a** and **11b**, could be isolated in its pure form after column chromatography. Importantly, only relatively slow rates of interconversion between the two atropisomers were observed above 60°C. The latter could thus be engaged in further reactions in their pure forms and were not subjected to significant re-equilibration during the subsequent synthetic steps. Reduction of the nitro functionality was conducted using zinc(0) in the presence of acetic acid at room temperature. Next, the amino-porphyrin **10a**(or **10b**) was acylated with chloroacetyl chloride at low temperature, followed by treatment of the resulting derivative **9a**(or **9b**) with 4-aza-18-crown-6 in gently refluxing methanol. Finally, saponification of the diester led to the desired ligands **2a**(or **2b**). In sharp contrast to ligands **1a** and **1b**, **2a** and **2b** were poorly soluble in most non-protic solvents in their free-base forms. Their solubility increased, however, after metalation with zinc. Therefore, only their zinc complexes will be considered in the following studies.

Detailed synthetic protocols for the preparation of ligands **1a**, **1b**, **2a**, **2b**, as well as for the reference compounds **R1**, and **R2** are described in the supporting information (*cf.* SI section 1).The conformations of ligands **1a**, **1b**, **2a** and **2b** were assigned using ^{1}H-NMR spectroscopy (*cf.* SI section 2.3 and 2.5 for the detailed analysis).

Calcium binding

^{1}H-NMR spectroscopy

The interaction of Ca^{2+} with the newly prepared *N,O*-class I and II ligands was probed using ^{1}H-NMR spectroscopy in MeOD containing 5% diisopropylethylamine (DIPEA). The organic base was introduced to ionize the carboxylic acid substituents, thus, permitting an optimal interaction of the ligand with Ca^{2+}. The choice of a bulky amine such as DIPEA was critical to avoid the formation of competitive inclusion complexes of the ammonium ions within the crown ether cavity and direct coordination to the zinc(II) center.

We initially focused on the atropisomers **1a** and **2a** only. For the first studies, aliquots of calcium chloride were added to 2 mM solutions of the porphyrins. In the case of ligand **1a** no (or only minor) evolution of the spectrum was observed at low Ca^{2+} concentration (< 10 mM), but gradual shifts of the peak positions were observed at higher Ca^{2+} concentrations (>20 mM), principally in the aromatic region (*cf.* SI section 2.7). These observations show that **1a** do not strongly interact with the Ca^{2+} ions. On the contrary, ligand **2a** exhibited dramatic perturbations of its spectrum in the presence of low concentrations of Ca^{2+} (< 1 mM) in both the aromatic and the aliphatic regions, suggesting the development of strong

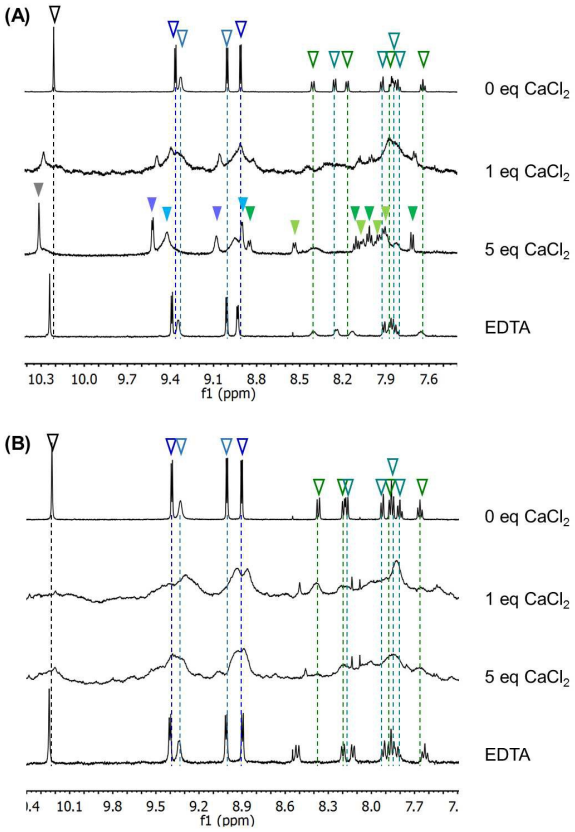

Figure 2: Effect of the addition of Ca^{2+} on the ^{1}H-NMR spectra of **2a** (A) and **2b** (B). The spectra were recorded for 2 mM solutions of the ligands in MeOD-5% diisopropylethylamine (DIPEA) at 298 K. The aliphatic region is not shown for clarity. Top spectra: free ligand (2 mM), and subsequent spectra recorded after the addition of 1 and 5 equivalents of $CaCl_2$. Bottom: spectra obtained after the addition of excess of ethylenediaminetetraacetic acid (EDTA). Note the growth of a sharp set of signals in the spectra of **2a** as compared to the rather broad massifs observed in the case of **2b** upon addition of Ca^{2+}. Triangles of identical color indicate spin systems exhibiting *J* coupling interactions in COSY experiments (*cf.* SI section 2.14); the vertical lines are added as a reference for the initial chemical shifts of the protons of the free ligands.

interactions with Ca^{2+} ions (see Figure 2A and *cf.* SI section 2.8). Therefore, extensive studies were conducted on class II *N,O*-ligands (**2a** and **2b**).

As shown in Figure 2, **2a** and **2b** are greatly affected by the addition of Ca^{2+} in solution (*cf.* SI sections 2.8 and 2.9 for spectra observed at intermediate Ca^{2+} concentrations). For both atropisomers the appearance of new sets of signals is observed, as well as a general broadening of the spectra which is indicative of the existence of dynamic exchange among the different species present in solution. The dynamic nature, and thus fully reversible interaction, between the Ca^{2+} and the porphyrin ligands was confirmed by the addition of a competing chelating agent, ethylenediaminetetraacetic acid (EDTA), which led to the recovery of the initial spectra for both ligands. Interestingly, while the introduction of Ca^{2+} results in a

View Article Online
DOI: 10.1039/C6DT04647A

Table 1: Characteristic rotational correlation times determined from time-resolved fluorescence anisotropy measurements of 2 mM solutions of ligands **2a** and **2b** in MeOH-5% DIPEA in presence of increasing amounts of calcium chloride. The samples were excited at 590 nm and the time-resolved fluorescence decays were recorded at 680 nm. The measurements were performed at 298 K (cf. SI section 3 for the decay traces and a detailed description of the measurements). ϑ_1, ϑ_2 and ϑ_3 are the rotational correlation times that fit best the experimental data, r_1, r_2 and r_3 are the pre-exponential factors (amplitudes) of each component used for the fitting (see SI section 3.1 Equation S2).

	2a				**2b**					
equiv. Ca^{2+}	ϑ_1 (ps)	$r_1(0)$	ϑ_2 (ns)	$r_2(0)$	ϑ_1 (ps)	$r_1(0)$	ϑ_2 (ns)	$r_2(0)$	ϑ_3 (ps)	$r_3(0)$
0	370 ± 10	0.12 ± 0.02	-	-	480 ± 10	0.17 ± 0.03	-	-	-	-
0.1	370 ± 10	0.13 ± 0.02	-	-	N/A	N/A	N/A	N/A	N/A	N/A
0.2	360 ± 10	0.13 ± 0.02	-	-	N/A	N/A	N/A	N/A	N/A	N/A
0.4	390 ± 10	0.15 ± 0.03	-	-	N/A	N/A	N/A	N/A	N/A	N/A
1	370[a]	0.10 ± 0.02	1.1 ± 0.1	0.04 ± 0.01	480[a]	0.08 ± 0.01	3.6 ± 0.7	0.01 ± 0.01	120 ± 20	0.03 ± 0.01
5	370[a]	0.11 ± 0.02	1.4 ± 0.1	0.06 ± 0.01	N/A	N/A	N/A	N/A	N/A	N/A

[a] fixed values; refer to the text for explanations.

general broadening and increase in complexity of the spectra of both atropisomers, the spectra of **2a** consistently exhibit sharper and simpler signal patterns. This is particularly noticeable for the addition of 1 to 5 equivalents of Ca^{2+}. In this concentration range, **2b** features broad and poorly resolved signals (see Figure 2B), whereas in the case of **2a** a distinct set of peaks emerges after the addition of 5 equivalents of Ca^{2+} (arrows Figure 2A). The assignment of this new set of peaks to a single, well defined species is further supported by the occurrence of a coherent spin-spin coupling pattern associated with these signals (*cf.* SI section 2.10). Collectively, these observations suggest that upon addition of 5 equivalents of Ca^{2+} the *cis*-atropisomer **2a** forms a dominant, discrete [porphyrin⊂Ca^{2+}], complex whereas for the *trans*-isomer **2b** a heterogeneous mixture of species in equilibrium is obtained.

In order to gain more insights into the nature of the species observed in the NMR experiments, time-resolved fluorescence anisotropy was used to investigate their hydrodynamic properties. The experimental conditions (solvent, concentration, temperature) were kept identical for both techniques to permit a fair comparison.

Time-resolved fluorescence anisotropy

*Free ligands (**2a** and **2b**)*

As shown in Table 1**,** in the absence of Ca^{2+}, each atropisomer exhibits a single-component anisotropy decay, with characteristic rotational correlation times of ϑ_1(**2a**) = (370 ± 10) ps and ϑ_1(**2b**) = (480 ± 10) ps (*cf.* SI sections 3.2 and 3.3). The difference observed between the rotation correlation times of **2a** and **2b** points towards a marked difference in their hydrodynamic properties (*i.e.* size, shape and solvatation *cf.* SI section 3.1, Equation S3), and is compatible with the observation of the two atropisomers.[99] Importantly, in the absence of Ca^{2+} the rotational correlation time of **2a** is not affected by dilution, confirming that free ligand does not aggregate in solution (*cf.* SI section 3.2).

*Evolution of the fluorescence anisotropy decay of ligand **2a** in the presence of Ca^{2+}*

Next, calcium chloride aliquots were added to the ligand solutions while keeping the concentration of porphyrin constant. In the case of the ligand **2a**, no major evolution of the fluorescence anisotropy decay is detected up to the addition of 0.4 equivalents of Ca^{2+} (*cf*. SI section 3.4). The system remains best described by a single-exponential decay in each case, and the rotational correlation times determined stay close to the value observed for the ligand alone (ϑ_1(**2a**) ~ 370 ps). The presence of complexed species under these conditions is, however, indicated by ^{1}H-NMR spectroscopy (*cf*. SI section 2.8). Therefore, minimal differences in the hydrodynamic properties of the complexed **[2a⊂Ca]** and the free ligand **2a** are inferred; the species present in solution remain undistinguishable by fluorescence anisotropy measurements, and ϑ_1(**2a**) ~ ϑ_1(**[2a⊂Ca]**) ~ 370 ps.[§] Notably, this observation points towards the formation of discrete mononuclear complexes between the calcium ions and the porphyrin ligand **2a** at low Ca^{2+} concentration. Upon increasing the Ca^{2+} concentration (≥ 1 equivalent added) a bi-exponential decay is required to describe the system (*cf*. SI section 3.4). In order to minimize the variables and the error in the determination of the rotational correlation times of the new species, the first component was fixed to the rotation time determined for the free/complexed monomeric ligands **2a**/**[2a⊂Ca]** (ϑ_1 ~ 370 ps). The second component of the fluorescence anisotropy decay is found to be significantly longer, with a rotational correlation time of ϑ_2 = (1.1 ± 0.1) ns. This observation indicates the formation of multimeric assemblies of the ligand **2a** at higher Ca^{2+} concentration. The appearance of an equilibrium between monomeric and multimeric porphyrin species in the presence of excess Ca^{2+} is

View Article Online
DOI: 10.1039/C6DT04647A

further supported by the observation of an even slower component in the fluorescence anisotropy decay after the addition of 5 equivalents of Ca^{2+}, with ϑ_2 = (1.4 ± 0.1) ns, which is indicative of the aggregation of **2a** into larger assemblies. This behavior reflects the multivalent nature of the crown ether and diacid moieties, both of which can lead to the development of coordination bonds with multiple cations and in different geometries. In the following the multimeric assemblies discussed above will be noted as **[2a$_x$⊂Ca$_n$]**.

*Evolution of the fluorescence anisotropy decay of ligand **2b** in the presence of Ca^{2+}*

Upon the addition of 1 equivalent of Ca^{2+}, the fluorescence anisotropy decay of **2b** is characterized by a triple exponential decay (Table 1; *cf*. SI section 3.5). Assuming the co-existence of different species in equilibrium, including monomeric **2b** species, one component was fixed to the rotational correlation time determined for the free ligand ϑ_1 ~ 480 ps. The two additional components are then characterized with rotation correlation times of ϑ_2= (3.6 ± 0.7) ns and ϑ_3 = (120 ± 20) ps respectively.[§§] The longest rotation correlation-time (ϑ_2) can be attributed to the presence of multimeric **[2b$_y$⊂Ca$_m$]** species in solution, resulting from calcium-induced aggregation of ligand **2b**. Interestingly, under identical conditions, ϑ_2(**[2b$_y$⊂Ca$_m$]**) was found to be significantly longer than ϑ_2(**[2a$_x$⊂Ca$_n$]**) (3.6 ns and 1.1 ns upon the addition of 1 equivalent of Ca^{2+} for **2b** and **2a**, respectively) pointing towards a higher propensity of the *trans*-atropisomer **2b** to form extended assemblies in the presence of divalent cations. This behavior can be explained by the antipodal orientation of the crown ether and diacid moieties in the latter atropisomer, and parallels the ^{1}H-NMR titration experiments discussed above. The observation of a shorter rotational correlation time (ϑ_3) is surprising, since an increase in the rotation speed of the ligand upon addition of Ca^{2+} would suggest an apparent decrease of its hydrodynamic radius. The occurrence of a rapid depolarization induced by Förster resonance energy transfer (FRET) within the extended porphyrin aggregates **[2b$_y$⊂Ca$_m$]** provides a possible explanation for the observation of this fast component in the fitting of the fluorescence anisotropy decay.[100] The occurrence of FRET in **2b** assemblies would suggest a mode of association which favors a close proximity of the chromophores within the assemblies, and clearly differs from the mode of association of the *cis*-atropisomer **2a** observed upon the addition of 1 equivalent of Ca^{2+}.

After having confirmed the preferential formation of discrete monomeric porphyrin complexes between the ligand **2a** and Ca^{2+} ions at low Ca^{2+} concentration, we turned to UV-Visible absorption spectroscopy to get an estimation of the association constant of the complexes in methanol.

UV-Visible absorption spectroscopy

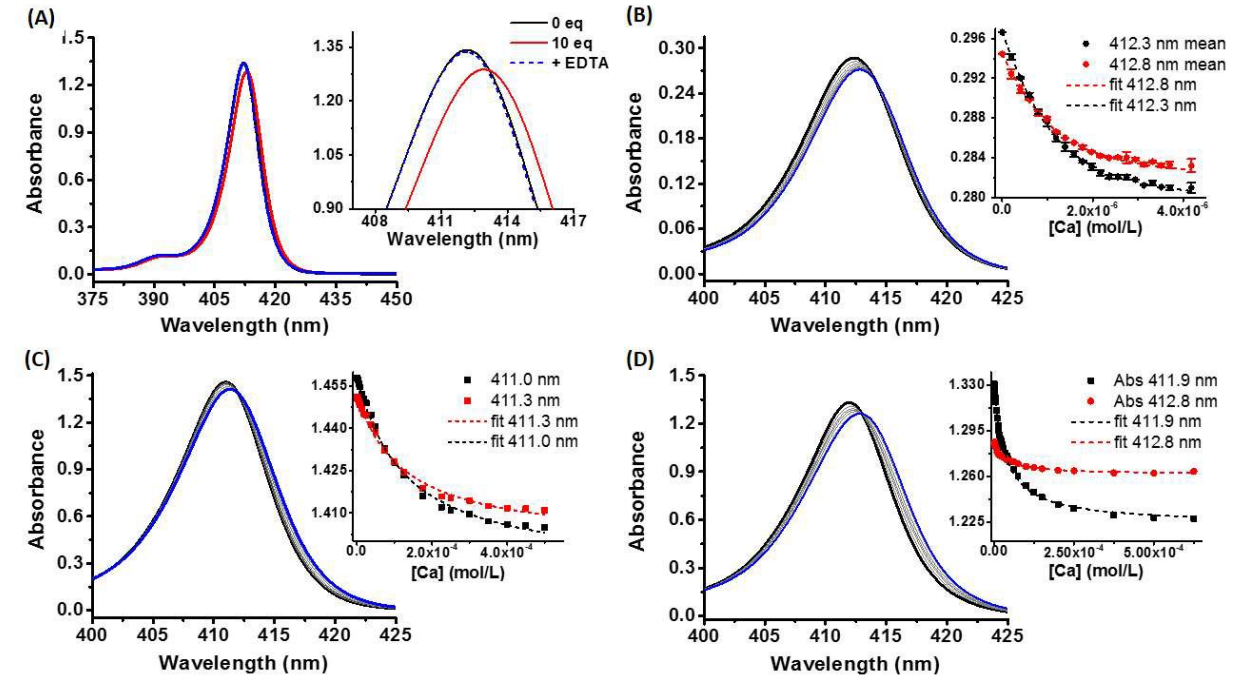

Figure 3: Evolution of the UV-Visible absorption spectra of ligands **2a**, **R2** and **8a** upon addition of Ca^{2+} in MeOH-5% DIPEA, at 298 K. (A) ~5 µM solution of **2a**; free ligand (solid black line); after addition of 10 equivalents of $CaCl_2$ (solid red line); after the addition of an excess of ethylenediaminetetraacetic acid (EDTA) (dashed blue line); inset: details of the Soret band. (B) ~ 1 µM solution of **2a** with the addition of 0 (black curve) to 4 equivalents of $CaCl_2$ (blue curve); inset: absorbance at 412.2 nm (black squares) and 412.8 nm (red circles) and corresponding fitted curves assuming the formation of a 1:1 **[2a⊂Ca]** complex. (C) ~2.5 µM solution of **R2** with the addition of 0 (black curve) to 180 (blue curve) equivalents of $CaCl_2$; inset: absorbance at 411.0 nm (black squares) and 411.3 nm (red squares) and corresponding fitted curves assuming the formation of a 1:1 **[R2⊂Ca]** complex. (D) ~2.5 µM solution of **8a** (see scheme 2) with the addition of 0 (black curve) to 250 (blue curve) equivalents of $CaCl_2$; inset: absorbance at 411.9 nm (black squares) and 412.8 nm (red squares) and corresponding fitted curves assuming the formation of a 1:1 **[2a⊂Ca]** complex.

View Article Online
DOI: 10.1039/C6DT04647A

*Ligand **2a***

As shown in Figure 3A and in the Supporting Information (*cf.* SI section 4.2), the addition of calcium chloride aliquots to a micromolar solution of **2a** induces a gradual shift of the ligand's spectrum, resulting in a slight red shift (0.6 nm) and a decrease in the absorption amplitude of the Soret band of the porphyrin. Addition of a competitor for binding the Ca^{2+} cations, namely EDTA, results in the recovery of the initial spectrum of **2a**, and confirms that the spectral evolution followed in these experiments is due to the specific interaction between **2a** and Ca^{2+} ions.

To limit the aggregation of the species observed by ^{1}H-NMR spectroscopy and fluorescence anisotropy measurements (experiments carried out in the millimolar range), the UV-Visible titration experiments were executed under high-dilution conditions (1 µM). At this concentration and with the addition of amounts up to 4.5 equivalents of Ca^{2+}, the maximum of the Soret band absorption shifts from 412.2 nm to 412.8 nm. Importantly, a well-defined isosbestic point centered at 414.1 nm is observed (*cf.* SI section 4.2), and implies the establishment of a simple equilibrium between the free ligand **2a** and a well-defined complex.[§§§] This observation suggests an initial bimolecular equilibrium, with the formation of simple 1:1 **[2a⊂Ca]** molecular complexes (*cf.* SI section 4.1, Equation S4). The evolution of the absorption of **2a** at 412.2 and 412.8 nm is well described using this simple model and leads to the estimation of an association constant of K_a (**2a**) ~ (2.4 ±0.2) x 10^6 M^{-1} for this first binding event (Figure 3B insert; *cf.* SI section 4.1).

In order to probe the degree of cooperativity between the crown ether and the diacid moieties for the complexation of Ca^{2+} by **2a**, the binding abilities of reference compounds **R1** and **R2** (Figure 1) and of the diester precursor **8a** (Scheme 2) were investigated as well.

*Reference ligands **R1, R2** and **8a***

In the case of **R1** which bears the diacid moiety only, slow precipitation of the ligand occurred upon addition of Ca^{2+} (*cf.* SI section 4.3), and therefore, no further analysis was conducted on this compound. It is worth noting that this behavior is reminiscent of the previously reported alkaline-earth induced aggregation of porphyrins bearing multiple carboxylic acids.[93] In sharp contrast, ligand **R2** bearing only a crown ether substituent was found competent for Ca^{2+} complexation. As was observed for **2a**, the addition of calcium chloride aliquots to a micromolar solution of **R2** induces a gradual shift of the spectrum of the ligand, which results in a minor red shift (0.3 nm) and slight decrease of the absorption intensity of the Soret band of the porphyrin (Figure 3C and *cf.* SI section 4.4).

The titration of a solution of **R2** at 2.5 µM in MeOH-5% DIPEA, with up to 180 equivalents of Ca^{2+}, leads to the gradual shifting of the maximum of the Soret band absorption from 411.0 nm to 411.3 nm. In that concentration range a well-defined isosbestic point centered at 411.9 nm is maintained (Figure 3C and *cf.* SI section 4.4). Increasing the ratio of Ca^{2+} to **R2** above 200 leads to the loss of the isosbestic point and suggests the occurrence of additional or competing coordination events at high Ca^{2+} concentration. Considering the large body of studies reporting the coordination of divalent cations by crown ether derivatives,[86-88] it is reasonable to assume that the first binding event (< 180 equivalents of Ca^{2+} added) corresponds to the formation of a simple 1:1 **[R2⊂Ca]** molecular complex. Thus, using the same model as above we obtain an estimated association constant of K_a(**R2**) ~ (8.1 ±0.4) x 10^3 M^{-1}).

Ligand **8a** behaved very similarly to **R2**. Upon addition of 0 to 250 equivalents of Ca^{2+} to a solution **8a** at 2.5 µM in MeOH-5% DIPEA, a modest red shift (0.9 nm) and decrease of the absorption intensity of the Soret-band is observed (Figure 3D). During the titration the maximum of the Soret-band absorption shifts from 411.9 nm to 412.8 nm. Furthermore, a well-defined isosbestic point appears at 413.0 nm, and suggests the occurrence of a simple equilibrium under the conditions tested (*cf.* SI section 4.5). For the same reason as before, we attributed this first event to the formation of a simple 1:1 **[8a⊂Ca]** molecular complex, and could estimate an association constant of K_a(**8a**) ~ (2.9 ±0.1) x 10^4 M^{-1}.

As summarized in Table 2 the UV-Visible titrations conducted on the reference (**R1**, **R2**, and **8a**) and target (**2a**) ligands, point towards a cooperative binding of Ca^{2+} by the diacid groups and the crown ether moiety in **2a**; the latter exhibiting the largest association constant of all the tested ligands. Importantly, for the structures and conditions investigated in the present work, the presence of the crown ether moiety is critical to avoid calcium-induced precipitation of the acid-functionalized porphyrins. The ester precursor of **2a** (*i.e.* **8a**) shows a surprisingly high affinity for Ca^{2+}, with an association constant K_a(**8a**) about one order of magnitude higher than K_a(**R2**) and two orders of magnitude lower than K_a(**2a**). Just as in the case of calcium-binding proteins, in which carbonyls groups from the peptidic backbone are frequently found in the coordination sphere of Ca^{2+},[84] it is plausible that for **8a**, the carbonyl oxygen atoms of the ester groups are involved in the cooperative binding of Ca^{2+} with the crown ether moiety and lead to the increase of the association constant as compared to **R2**. Furthermore, it is interesting to note that **8a** shows very little tendency to aggregate or diverge from a simple binding isotherm during the titration with Ca^{2+}.

Table 2: Association constants for the first elemental Ca^{2+} complexation event observed for micromolar solutions of **R1**, **R2**, **8a**, and **2a**, in MeOH containing 5% of DIPEA at 298 K.

Ligand	R1	R2	8a	2a
K_a (M^1)	n/a[a]	8.1 ±0.4 x 10^3	2.9 ±0.1 x 10^4	2.4 ±0.2 x 10^6

[a] No association constant estimated due to precipitation of the ligand upon exposure to Ca^{2+}. [b] Determined from 2.5 µM ligand solution in MeOH-5% DIPEA, upon addition of 0 to 180 equivalents of Ca^{2+}. [c] Determined from 2.5 µM ligand solution in MeOH-5% DIPEA upon addition of 0 to 250 equivalents of Ca^{2+}. [d] Determined from a 1 µM ligand solution in MeOH-5% DIPEA upon the addition of 0 to 4 equivalents of Ca^{2+}.

View Article Online
DOI: 10.1039/C6DT04647A

A robust isosbestic point is observed, even at high Ca^{2+} to **8a** ratios (up to 250) and supports the establishment of a simple equilibrium between two well-defined species (presumably [**8a**] and [**8a⊂Ca**]). This contrasts with the more complex behavior observed for **2a**, which rapidly diverges from a single equilibrium at high concentration of Ca^{2+} and/or of the ligand. However, despite this slightly more complex behavior, the introduction of ionizable groups within the ligand scaffold (*i.e.*, the carboxylic acids groups) increases the association constant with Ca^{2+} by two orders of magnitude, which is expected for ligands that are able to provide charge compensation upon complexation.[87, 88] The enhanced association constant observed for **2a** is of particular relevance for using this class of ligands in aqueous environment. Indeed, the association constants between macrocyclic ligands and alkaline and alkaline-earth cations are three to four orders of magnitude larger in pure methanol than in water, due to the decrease in the desolvation enthalpy of the cations in solvents of lower dielectric constant.[87, 88] Thus **2a** represents a promising scaffold for building ligands for the assembly of discrete transition metal/alkaline-earth hetero-metallic complexes in aqueous conditions.

Conclusions

The introduction of crown ether and carboxylic acid substituents on porphyrin macrocycles is a fruitful strategy for building a secondary binding site for oxophilic cations in the apical position of the N_4-chelating motif of porphyrins. In this work we used this strategy to design a versatile class of bitopic *N,O*-ligands, able to drive the formation of stable transition metal/alkaline-earth hetero-metallic complexes in solution. As a proof of principle, we characterized the association of Zn^{2+} and Ca^{2+} cations in protic media.

We demonstrated that the use of semi-flexible oxygen rich substituents is critical for the design of a competent binding site for labile alkaline-earth cations at the periphery of the rigid porphyrin macrocycle. It is likely that the introduction of flexible, partly pre-organized, binding motif is advantageous because the binding pocket remains free to reorganize in order to optimize its interaction with the desired cations. This approach led us to the synthesis of a ligand exhibiting a moderately large association constant with the labile Ca^{2+} (K_a(**2a**) ~ 2.4 (±0.2) x 10^6 M^{-1}) in methanol. This result is encouraging for the development of fully water soluble ligands based on the same binding motifs and the association of alkaline-earth cations and transition metals within a compact organic scaffold in aqueous environment. Importantly, the cooperative binding of Ca^{2+} by the crown ether and the diacid moiety grafted on two opposite *meso*-positions of the porphyrin macrocycle in **2a** implies the binding of the Ca^{2+} in the apical position of the N_4-chelating motif of the porphyrin and in close proximity to a metal atom chelated by the porphyrin macrocycle.

This work introduces a general class of bitopic *N,O*-ligands, providing a promising base to study the emergence of cooperativity and synergism between transition metals and alkaline-earth metals in discrete heterometalic assemblies. Operating in protic media, these constructs can provide frameworks for developing bio-inspired catalytic systems such as the water oxidizing complex in photosynthesis. Indeed, after suitable functionalization porphyrins complexes are amenable to electrocatalysis at significantly positive potentials.

Acknowledgements

The work at ASU was supported by the Center for Bio-Inspired Solar Fuel Production, an Energy Frontier Research Center funded by the U.S. Department of Energy, Office of Science, Office of Basic Energy Sciences under Award Number DESC0001016, and the Office of Basic Energy Sciences, Division of Chemical Sciences, Geosciences, and Energy Biosciences, Department of Energy under contract DE-FG02-03ER15393.

Notes and references

§ The presence of free and complexed species of quasi identical hydrodynamic radius is further supported by experiments conducted at low concentration. For a 0.1 mM solution of **2a** in MeOH-5% DIPEA, at 298 K, and in the presence of 0.1 mM of $CaCl_2$, the fluorescence anisotropy decay of the porphyrin remains best fitted with a single exponential decay with a life time of 370 ps. In similar conditions the ^{1}H NMR spectrum exhibits a well-defined set of peaks that can be attributed to monomeric complexed species, *cf*. SI section 3.2 (anisotropy) and section 2.11 (^{1}H NMR).

§§ The fitting of the anisotropy decay of **2b** in the presence of Ca^{2+} with three floating variables led to values of the three components reasonably close to those determined upon fixing one component to the rotation correlation time of the monomeric ligand (*cf*. SI section 3.5).

§§§ Upon addition of more Ca^{2+}, or in presence of a higher concentration of the ligand, the isosbestic point was rapidly lost and no meaningful fitting could be undertaken.

1. J. M. Lehn, *Pure Appl. Chem.*, 1980, **52**, 2441-2459.
2. J. M. Lehn, *Angew. Chem. Int. Ed.*, 11000, **29**, 1304-1319.
3. E. K. van den Beuken and B. L. Feringa, *Tetrahedron*, 1998, **54**, 12985-13011.
4. M. Jarenmark, H. Carlsson and E. Nordlander, *C. R. Chim.*, 2007, **10**, 433-462.
5. M. Shibasaki, M. Kanai, S. Matsunaga and N. Kumagai, *Acc. Chem. Res.*, 2009, **42**, 1117-1127.
6. S. K. Mandal and H. W. Roesky, *Acc. Chem. Res.*, 2010, **43**, 248-259.
7. B. G. Cooper, J. W. Napoline and C. M. Thomas, *Catal. Rev.*, 2012, **54**, 1-40.
8. J. A. Mata, F. E. Hahn and E. Peris, *Chem. Sci.*, 2014, **5**, 1723-1732.
9. S. Matsunaga and M. Shibasaki, *Chem. Commun.*, 2014, **50**, 1044-1057.
10. P. Buchwalter, J. Rosé and P. Braunstein, *Chem. Rev.*, 2015, **115**, 28-126.
11. A. Mittasch, *Geschichte der Ammoniaksynthese*, Verlag Chemie, [Weinheim (Bergstrasse), 1951.
12. W. D. Mross, *Catal. Rev.*, 1983, **25**, 591-637.
13. H. P. Bonzel, *J. Vac. Sci. Technol. A*, 1984, **2**, 866-872.
14. M. Hammouche, D. Lexa, M. Momenteau and J. M. Saveant, *J. Am. Chem. Soc.*, 1991, **113**, 8455-8466.

View Article Online
DOI: 10.1039/C6DT04647A

15. C. G. Miller, S. W. Gordon-Wylie, C. P. Horwitz, S. A. Strazisar, D. K. Peraino, G. R. Clark, S. T. Weintraub and T. J. Collins, *J. Am. Chem. Soc.*, 1998, **120**, 11540-11541.
16. C.-I. Lee, K. V. Lakshmi and G. W. Brudvig, *Biochemistry*, 2007, **46**, 3211-3223.
17. G. W. Brudvig, *Phil. Trans. R. Soc. B*, 2008, **363**, 1211-1218.
18. B. E. Koel and J. Kim, in *Handbook of Heterogeneous Catalysis*, Wiley-VCH Verlag GmbH & Co. KGaA, 2008, DOI: 10.1002/9783527610044.hetcat0087.
19. C. F. Yocum, *Coord. Chem. Rev.*, 2008, **252**, 296-305.
20. C. Ratnasamy and J. P. Wagner, *Catal. Rev.*, 2009, **51**, 325-440.
21. S. Fukuzumi, Y. Morimoto, H. Kotani, P. Naumov, Y.-M. Lee and W. Nam, *Nat. Chem.*, 2010, **2**, 756-759.
22. M. M. Najafpour, T. Ehrenberg, M. Wiechen and P. Kurz, *Angew. Chem. Int. Ed.*, 2010, **49**, 2233-2237.
23. Y. Zhai, D. Pierre, R. Si, W. Deng, P. Ferrin, A. U. Nilekar, G. Peng, J. A. Herron, D. C. Bell, H. Saltsburg, M. Mavrikakis and M. Flytzani-Stephanopoulos, *Science*, 2010, **329**, 1633-1636.
24. N. Cox, L. Rapatskiy, J.-H. Su, D. A. Pantazis, M. Sugiura, L. Kulik, P. Dorlet, A. W. Rutherford, F. Neese, A. Boussac, W. Lubitz and J. Messinger, *J. Am. Chem. Soc.*, 2011, **133**, 14149-14149.
25. J. S. Kanady, E. Y. Tsui, M. W. Day and T. Agapie, *Science*, 2011, **333**, 733-736.
26. Y. Morimoto, H. Kotani, J. Park, Y.-M. Lee, W. Nam and S. Fukuzumri, *J. Am. Chem. Soc.*, 2011, **133**, 403-405.
27. S. Nayak, H. P. Nayek, S. Dehnen, A. K. Powell and J. Reedijk, *Dalton Trans.*, 2011, **40**, 2699-2702.
28. J. Park, Y. Morimoto, Y.-M. Lee, Y. You, W. Nam and S. Fukuzumi, *Inorg. Chem.*, 2011, **50**, 11612-11622.
29. Y. J. Park, J. W. Ziller and A. S. Borovik, *J. Am. Chem. Soc.*, 2011, **133**, 9258-9261.
30. F. F. Pfaff, S. Kundu, M. Risch, S. Pandian, F. Heims, I. Pryjomska-Ray, P. Haack, R. Metzinger, E. Bill, H. Dau, P. Comba and K. Ray, *Angew. Chem. Int. Ed.*, 2011, **50**, 1711-1715.
31. V. K. Yachandra and J. Yano, *J. Photochem. Photobiol. B*, 2011, **104**, 51-59.
32. I. Zaharieva, M. M. Najafpour, M. Wiechen, M. Haumann, P. Kurz and H. Dau, *Energ. Environ. Sci.*, 2011, **4**, 2400-2408.
33. Y. Morimoto, J. Park, T. Suenobu, Y.-M. Lee, W. Nam and S. Fukuzumi, *Inorg. Chem.*, 2012, **51**, 10025-10036.
34. M. Wiechen, I. Zaharieva, H. Dau and P. Kurz, *Chem. Sci.*, 2012, **3**, 2330-2339.
35. J. Chen, Y.-M. Lee, K. M. Davis, X. Wu, M. S. Seo, K.-B. Cho, H. Yoon, Y. J. Park, S. Fukuzumi, Y. N. Pushkar and W. Nam, *J. Am. Chem. Soc.*, 2013, **135**, 6388-6391.
36. L. Dong, Y. Wang, Y. Lv, Z. Chen, F. Mei, H. Xiong and G. Yin, *Inorg. Chem.*, 2013, **52**, 5418-5427.
37. J. S. Kanady, J. L. Mendoza-Cortes, E. Y. Tsui, R. J. Nielsen, W. A. Goddard, III and T. Agapie, *J. Am. Chem. Soc.*, 2013, **135**, 1073-1082.
38. Y. J. Park, S. A. Cook, N. S. Sickerman, Y. Sano, J. W. Ziller and A. S. Borovik, *Chem. Sci.*, 2013, **4**, 717-726.
39. E. Y. Tsui and T. Agapie, *Proc. Natl. Acad. Sci. U. S. A.*, 2013, **110**, 10084-10088.
40. E. Y. Tsui, R. Tran, J. Yano and T. Agapie, *Nat. Chem.*, 2013, **5**, 293-299.
41. K. Yamaguchi, S. Yamanaka, H. Isobe, T. Saito, K. Kanda, Y. Umena, K. Kawakami, J. R. Shen, N. Kamiya, M. Okumura, H. Nakamura, M. Shoji and Y. Yoshioka, *Int. J. Quantum Chem.*, 2013, **113**, 453-473.
42. H. Yoon, Y.-M. Lee, X. Wu, K.-B. Cho, R. Sarangi, W. Nam and S. Fuhkuzumi, *J. Am. Chem. Soc.*, 2013, **135**, 9186-9194.
43. J. Park, Y. Morimoto, Y.-M. Lee, W. Nam and S. Fukuzumi, *Inorg. Chem.*, 2014, **53**, 3618-3628.
44. Y.-M. Lee, S. Bang, Y. M. Kim, J. Cho, S. Hong, T. Nomura, T. Ogura, O. Troeppner, I. Ivanovic-Burmazovic, R. Sarangi, S. Fukuzumi and W. Nam, *Chem. Sci.*, 2013, **4**, 3917-3923.
45. S. Bang, Y.-M. Lee, S. Hong, K.-B. Cho, Y. Nishida, M. S. Seo, R. Sarangi, S. Fukuzumi and W. Nam, *Nat Chem*, 2014, **6**, 934-940.
46. Z. Zhang, K. L. Coats, Z. Chen, T. J. Hubin and G. Yin, *Inorg. Chem.*, 2014, **53**, 11937-11947.
47. D. E. Herbert, D. Lionetti, J. Rittle and T. Agapie, *J. Am. Chem. Soc.*, 2013, **135**, 19075-19078.
48. P.-H. Lin, M. K. Takase and T. Agapie, *Inorg. Chem.*, 2015, **54**, 59-64.
49. S. Fukuzumi, K. Ohkubo, Y.-M. Lee and W. Nam, *Chemistry – A European Journal*, 2015, **21**, 17548-17559.
50. J. S. Vrettos, D. A. Stone and G. W. Brudvig, *Biochemistry*, 2001, **40**, 7937-7945.
51. G. Hendry and T. Wydrzynski, *Biochemistry*, 2003, **42**, 6209-6217.
52. C. I. Lee, K. V. Lakshmi and G. W. Brudvig, *Biochemistry*, 2007, **46**, 3211-3223.
53. N. Cox, L. Rapatskiy, J. H. Su, D. A. Pantazis, M. Sugiura, L. Kulik, P. Dorlet, A. W. Rutherford, F. Neese, A. Boussac, W. Lubitz and J. Messinger, *J. Am. Chem. Soc.*, 2011, **133**, 3635-3648.
54. M. M. Najafpour, *Dalton Trans.*, 2011, **40**, 3793-3795.
55. J. Cho, S. Jeon, S. A. Wilson, L. V. Liu, E. A. Kang, J. J. Braymer, M. H. Lim, B. Hedman, K. O. Hodgson, J. S. Valentine, E. I. Solomon and W. Nam, *Nature*, 2011, **478**, 502-505.
56. C. Choe, L. Yang, Z. Lv, W. Mo, Z. Chen, G. Li and G. Yin, *Dalton Trans.*, 2015, **44**, 9182-9192.
57. F. Li, K. M. Van Heuvelen, K. K. Meier, E. Münck and L. Que, *J. Am. Chem. Soc.*, 2013, **135**, 10198-10201.
58. S. Mukherjee, J. A. Stull, J. Yano, T. C. Stamatatos, K. Pringouri, T. A. Stich, K. A. Abboud, R. D. Britt, V. K. Yachandra and G. Christou, *Proc. Natl. Acad. Sci. U. S. A.*, 2012, **109**, 2257-2262.
59. C. Zhang, C. Chen, H. Dong, J.-R. Shen, H. Dau and J. Zhao, *Science*, 2015, **348**, 690-693.
60. R. C. Cammarota and C. C. Lu, *J. Am. Chem. Soc.*, 2015, **137**, 12486-12489.
61. Y. Umena, K. Kawakami, J.-R. Shen and N. Kamiya, *Nature*, 2011, **473**, 55-U65.
62. A. Mishra, W. Wernsdorfer, K. A. Abboud and G. Christou, *Chem. Commun.*, 2005, DOI: 10.1039/b413680b, 54-56.
63. I. J. Hewitt, J.-K. Tang, N. T. Madhu, R. Clerac, G. Buth, C. E. Anson and A. K. Powell, *Chem. Commun.*, 2006, DOI: 10.1039/b518026k, 2650-2652.
64. A. Mishra, J. Yano, Y. Pushkar, V. K. Yachandra, K. A. Abboud and G. Christou, *Chem. Commun.*, 2007, DOI: 10.1039/b701355h, 1538-1540.
65. M. U. Anwar, L. N. Dawe and L. K. Thompson, *Dalton Trans.*, 2011, **40**, 8079-8082.

View Article Online
DOI: 10.1039/C6DT04647A

66. V. Kotzabasaki, M. Siczek, T. Lis and C. J. Milios, *Inorg. Chem. Commun.*, 2011, **14**, 213-216.
67. E. S. Koumousi, S. Mukherjee, C. M. Beavers, S. J. Teat, G. Christou and T. C. Stamatatos, *Chem. Commun.*, 2011, **47**, 11128-11130.
68. A. A. Alaimo, D. Takahashi, L. Cunha-Silva, G. Christou and T. C. Stamatatos, *Inorg. Chem.*, 2015, **54**, 2137-2151.
69. R. O. Fuller, G. A. Koutsantonis, I. Lozic, M. I. Ogden and B. W. Skelton, *Dalton Trans.*, 2015, **44**, 2132-2137.
70. A. C. Benniston, S. Melnic, C. Turta, A. B. Arauzo, J. Bartolome, E. Bartolome, R. W. Harrington and M. R. Probert, *Dalton Trans.*, 2014, **43**, 13349-13357.
71. B. Gerey, M. Gennari, E. Goure, J. Pecaut, A. Blackman, D. A. Pantazis, F. Neese, F. Molton, J. Fortage, C. Duboc and M.-N. Collomb, *Dalton Trans.*, 2015, **44**, 12757-12770.
72. J. S. Kanady, R. Tran, J. A. Stull, L. Lu, T. A. Stich, M. W. Day, J. Yano, R. D. Britt and T. Agapie, *Chem. Sci.*, 2013, **4**, 3986-3996.
73. K. M. S. K. M. G. R. Kadish, *The porphyrin handbook. Vol.3, Inorganic, organometallic and coordination chemistry*, Academic, San Diego, Calif. ; London, 2000.
74. J. W. Buchler, *J. Porphyrins Phthalocyanines*, 2000, **4**, 337-339.
75. C. M. Lemon, D. K. Dogutan and D. G. Nocera, in *Handbook of Porphyrin Science*, DOI: doi:10.1142/9789814397605_0001, pp. 1-143.
76. E. Rose, B. Andrioletti, S. Zrig and M. Quelquejeu-Ehteve, *Chem. Soc. Rev.*, 2005, **34**, 573-583.
77. J. Rosenthal and D. G. Nocera, in *Progress in Inorganic Chemistry, Vol 55*, ed. K. D. Karlin, 2007, vol. 55, pp. 483-544.
78. M. M. Abu-Omar, *Dalton Trans.*, 2011, **40**, 3435-3444.
79. D. Wang and J. T. Groves, *Proc. Natl. Acad. Sci. U. S. A.*, 2013, **110**, 15579-15584.
80. C. Costentin, M. Robert, J.-M. Savéant and A. Tatin, *Proc. Natl. Acad. Sci. U. S. A.*, 2015, **112**, 6882-6886.
81. C. T. Carver, B. D. Matson and J. M. Mayer, *J. Am. Chem. Soc.*, 2012, **134**, 5444-5447.
82. L. Bonomo, M. L. Lehaire, E. Solari, R. Scopelliti and C. Floriani, *Angew. Chem. Int. Ed.*, 2001, **40**, 771-774.
83. J. J. Falke, S. K. Drake, A. L. Hazard and O. B. Peersen, *Q. Rev. Biophys.*, 1994, **27**, 219-290.
84. A. K. Katz, J. P. Glusker, S. A. Beebe and C. W. Bock, *J. Am. Chem. Soc.*, 1996, **118**, 5752-5763.
85. P. G. Daniele, C. Foti, A. Gianguzza, E. Prenesti and S. Sammartano, *Coord. Chem. Rev.*, 2008, **252**, 1093-1107.
86. B. Dietrich, *J. Chem. Educ.*, 1985, **62**, 954-964.
87. R. M. Izatt, K. Pawlak, J. S. Bradshaw and R. L. Bruening, *Chem. Rev.*, 1991, **91**, 1721-2085.
88. R. M. Izatt, K. Pawlak, J. S. Bradshaw and R. L. Bruening, *Chem. Rev.*, 1995, **95**, 2529-2586.
89. K. M. Fromm, *Coord. Chem. Rev.*, 2008, **252**, 856-885.
90. P. Even and B. Boitrel, *Coord. Chem. Rev.*, 2006, **250**, 519-541.
91. Z. Gross and I. Toledano, *J. Org. Chem.*, 1994, **59**, 8312-8315.
92. B. Boitrel, Z. Halime, L. Michaudet, M. Lachkar and L. Toupet, *Chem. Commun.*, 2003, DOI: 10.1039/b309615g, 2670-2671.
93. Y. Uemori, A. Osada, H. Munakata and H. Imai, *Inorg. Chim. Acta*, 2006, **359**, 4594-4600.
94. N. Rusakova, N. Semenishyn and Y. Korovin, *J. Porphyrins Phthalocyanines*, 2010, **14**, 166-169.
95. S. Le Gac and B. Boitrel, *J. Porphyrins Phthalocyanines*, 2012, **16**, 537-544.
96. S. Le Gac, L. Fusaro, T. Roisnel and B. Boitrel, *J. Am. Chem. Soc.*, 2014, **136**, 6698-6715.
97. Z. Halime, M. Lachkar, L. Toupet, A. G. Coutsolelos and B. Boitrel, *Dalton Trans.*, 2007, DOI: 10.1039/b701889d, 3684-3689.
98. C. Comte, C. P. Gros, S. Koeller, R. Guilard, D. J. Nurco and K. M. Smith, *New J. Chem.*, 1998, **22**, 621-626.
99. P. J. W. Debye, *Polar molecules*, The Chemical Catalog Company, inc., New York, 1929.
100. B. Valeur and M. N. Berberan-Santos, *Molecular Fluorescence: Principles and Applications*, Wiley, 2012.